Science Advances
AAAS

Supplementary Materials for

RAD51AP2 is required for efficient meiotic recombination between X and Y chromosomes

Hui Ma, Tao Li, Xuefeng Xie, Long Jiang, Jingwei Ye, Chenjia Gong, Hanwei Jiang, Suixing Fan, Huan Zhang, Baolu Shi, Beibei Zhang, Xiaohua Jiang, Yang Li, Jianteng Zhou, Jianze Xu, Xingxia Zhang, Xiaoning Hou, Hao Yin*, Yuanwei Zhang*, Qinghua Shi*

*Corresponding author. Email: qshi@ustc.edu.cn (Q.S.); zyuanwei@ustc.edu.cn (Y.Z.); yh213@ustc.edu.cn (H.Y.).

Published 12 January 2022, *Sci. Adv.* **8**, eabk1789 (2022)
DOI: 10.1126/sciadv.abk1789

This PDF file includes:

Supplementary Figure 1

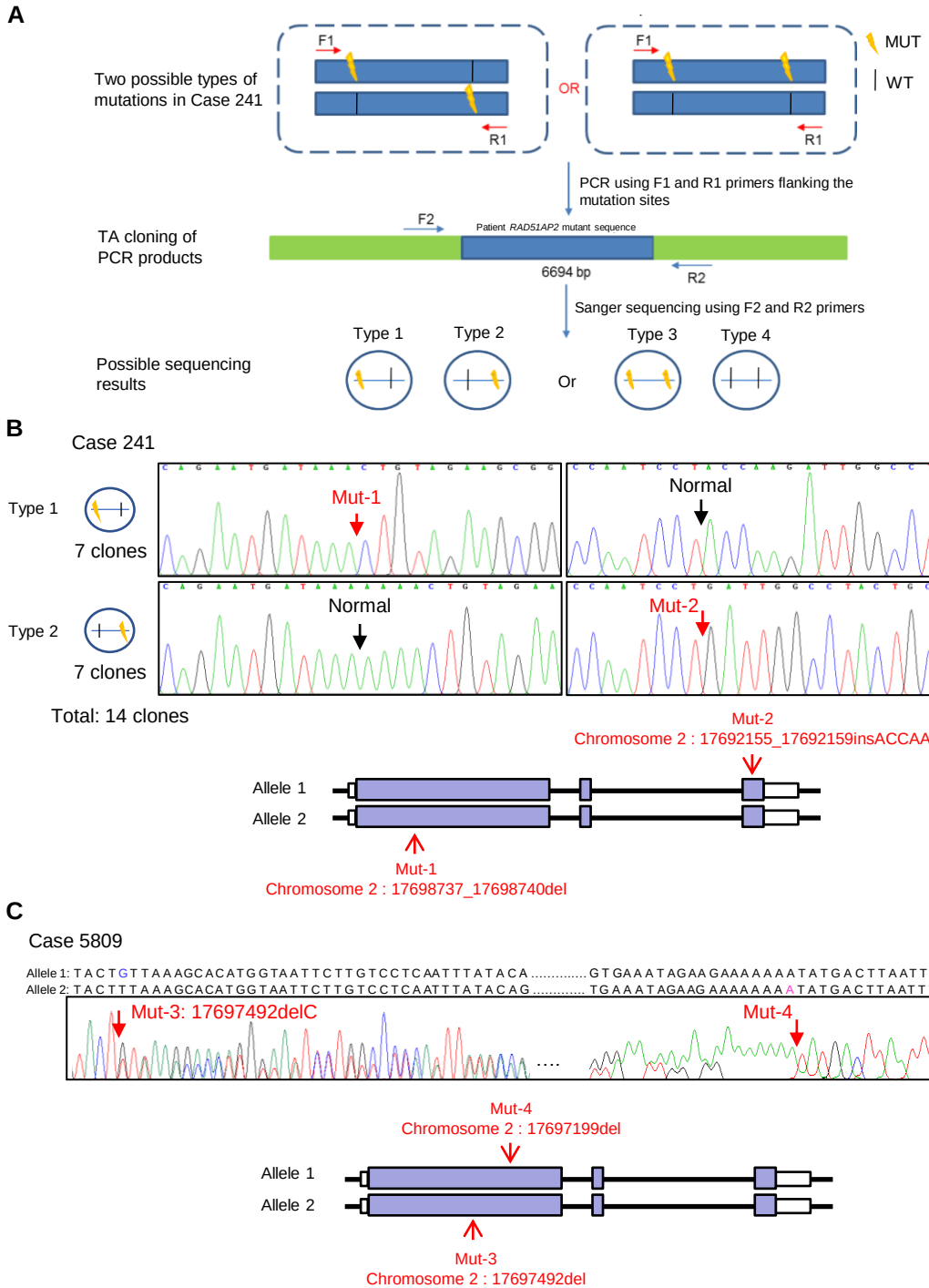

Fig. S1. Patients have compound heterozygous *RAD51AP2* mutations. (**A**) Schematic diagram showing the TA cloning of the mutations identified in Case 241. PCR using primers flanking the two mutation sites of *RAD51AP2* was conducted with genomic DNA (gDNA) from blood samples of the case and PCR products (6694 kb) were inserted into T vectors, followed by Sanger sequencing of colonies. The sequencing results could be one of these two combinations: in one combination, each plasmid contains only one mutation (type 1 and type 2), indicating that the two mutations lie on different chromosomes; In the other combination, one plasmid contains no mutation and one plasmid contains two mutations (type 3 and type 4), indicating that the two mutations lie on the same chromosome. (**B**) Representative Sanger sequencing chromatograms of the *RAD51AP2* mutations sites in T vectors inserted with the PCR products from Case 241. Sanger sequencing results of a total of 14 clones: 7 clones only contained the *RAD51AP2* mutation c. 943-946delTTTT (type 1) and the other 7 clones only contained the mutation c.3391-3395insTTGGT (type 2). Red arrows indicate mutation sites and black arrows indicate sites containing no mutations. (**C**) A representative Sanger sequencing chromatogram of the *RAD51AP2* mutations in genomic DNA of blood samples from Case 5809. Purple boxes indicate the exons. Red arrows indicate the mutation sites.

Supplementary Figure 2

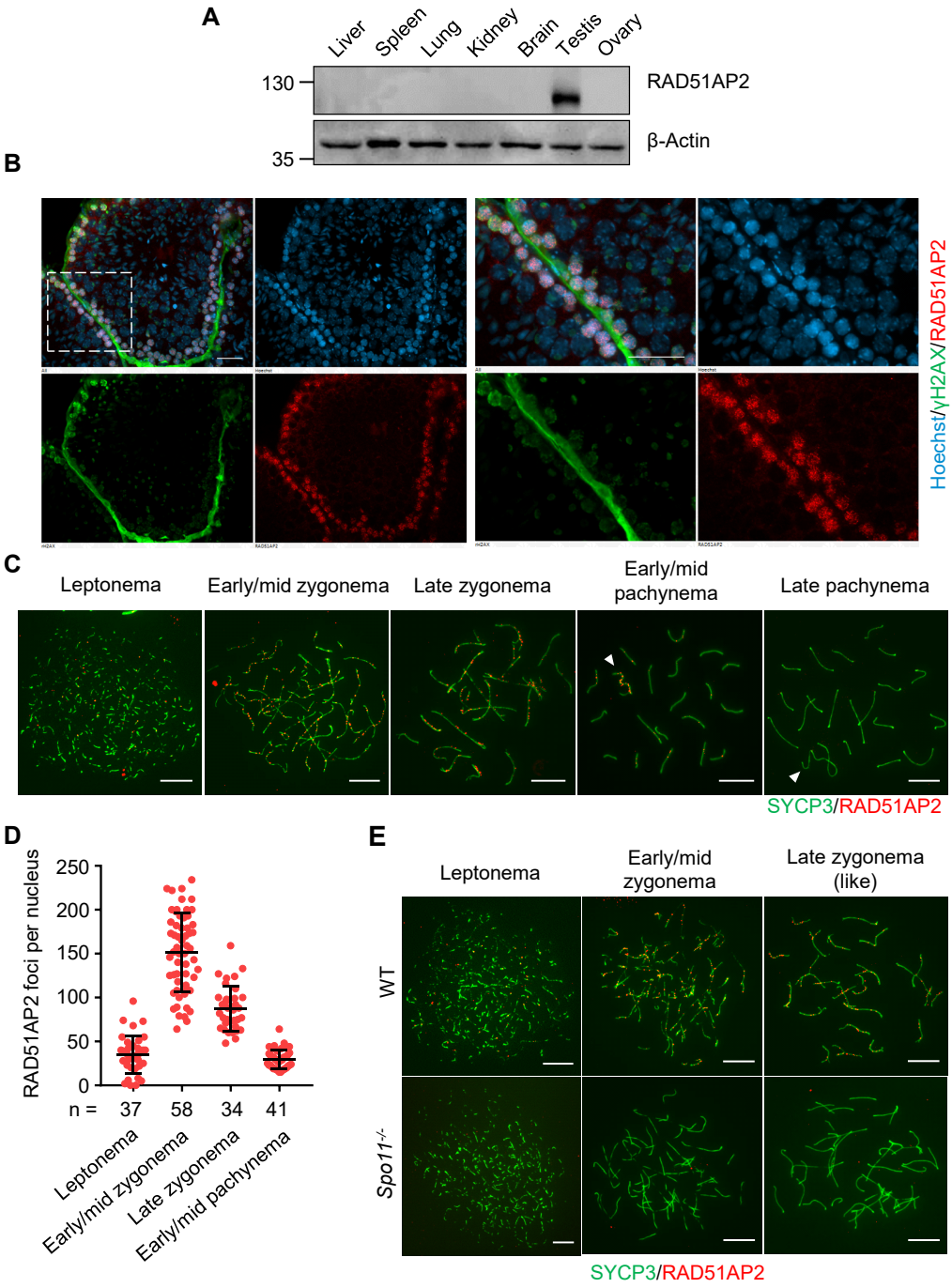

Supplementary Figure 3

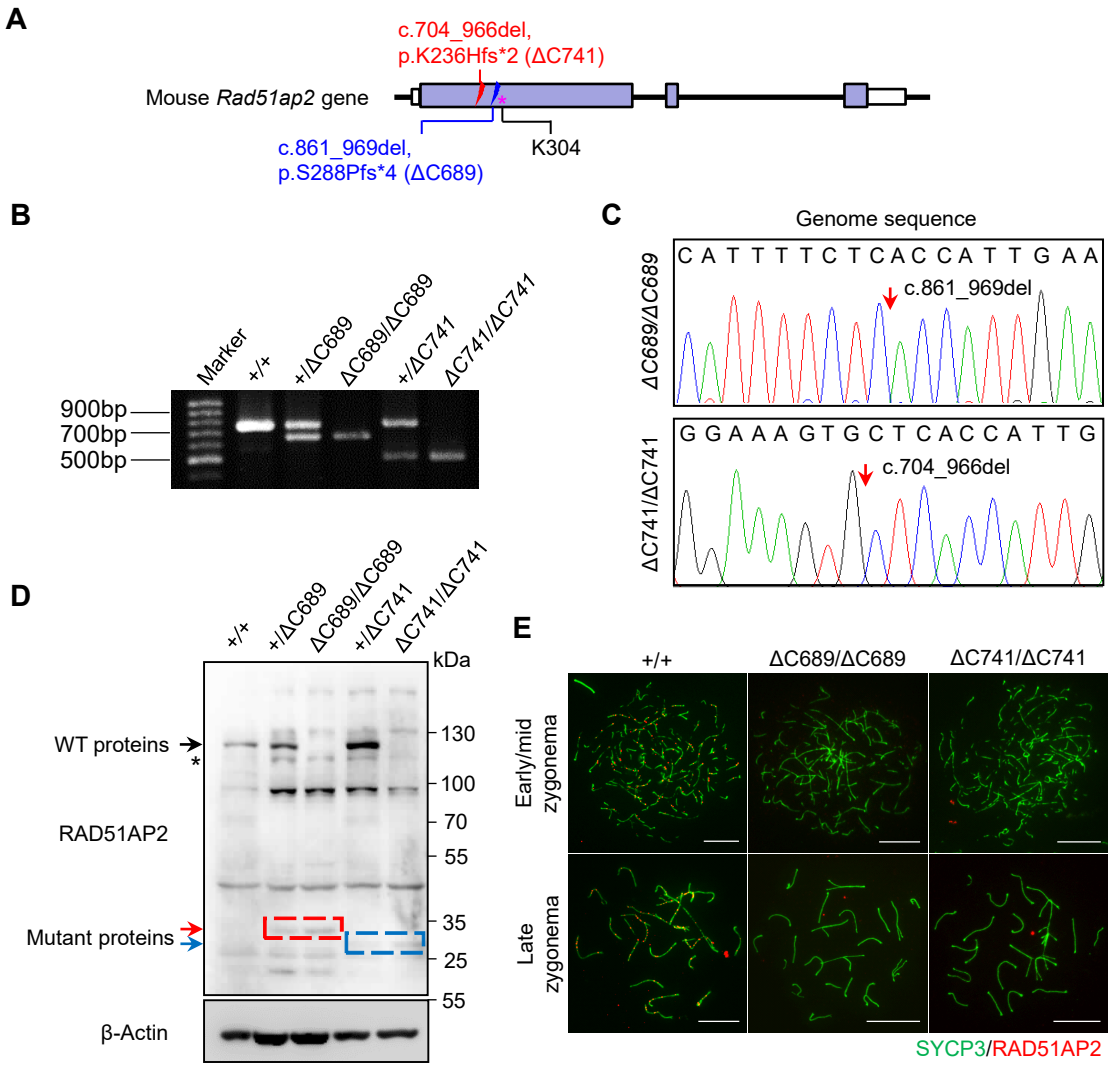

Fig. S3. Generation of *Rad51ap2* mutant mice. (**A**) Diagram of the mouse *Rad51ap2* locus showing the mutation sites in the two *Rad51ap2* mutant lines. The lightning signs indicate the mutation sites in the two lines. The mutation site, corresponding to the Mut-1 in case 241, is indicated by the pink asterisk. (**B**, **C**) The mutations in the two *Rad51ap2* mutant mouse lines were confirmed by PCR (**B**) and Sanger sequencing (**C**) of the genomic DNAs. Arrows indicate the mutation sites. (**D**) Detection of the RAD51AP2 proteins in testes from the *Rad51ap2* mutant mouse lines. β-Actin was used as the loading control. Arrows, bands corresponding to the WT or truncating RAD51AP2 proteins. Asterisk, a non-specific band. (**E**) Representative spread spermatocytes from the WT and *Rad51ap2* mutant mice stained for RAD51AP2 (red) and SYCP3 (green). Scale bars, 10 μm.

Supplementary Figure 4

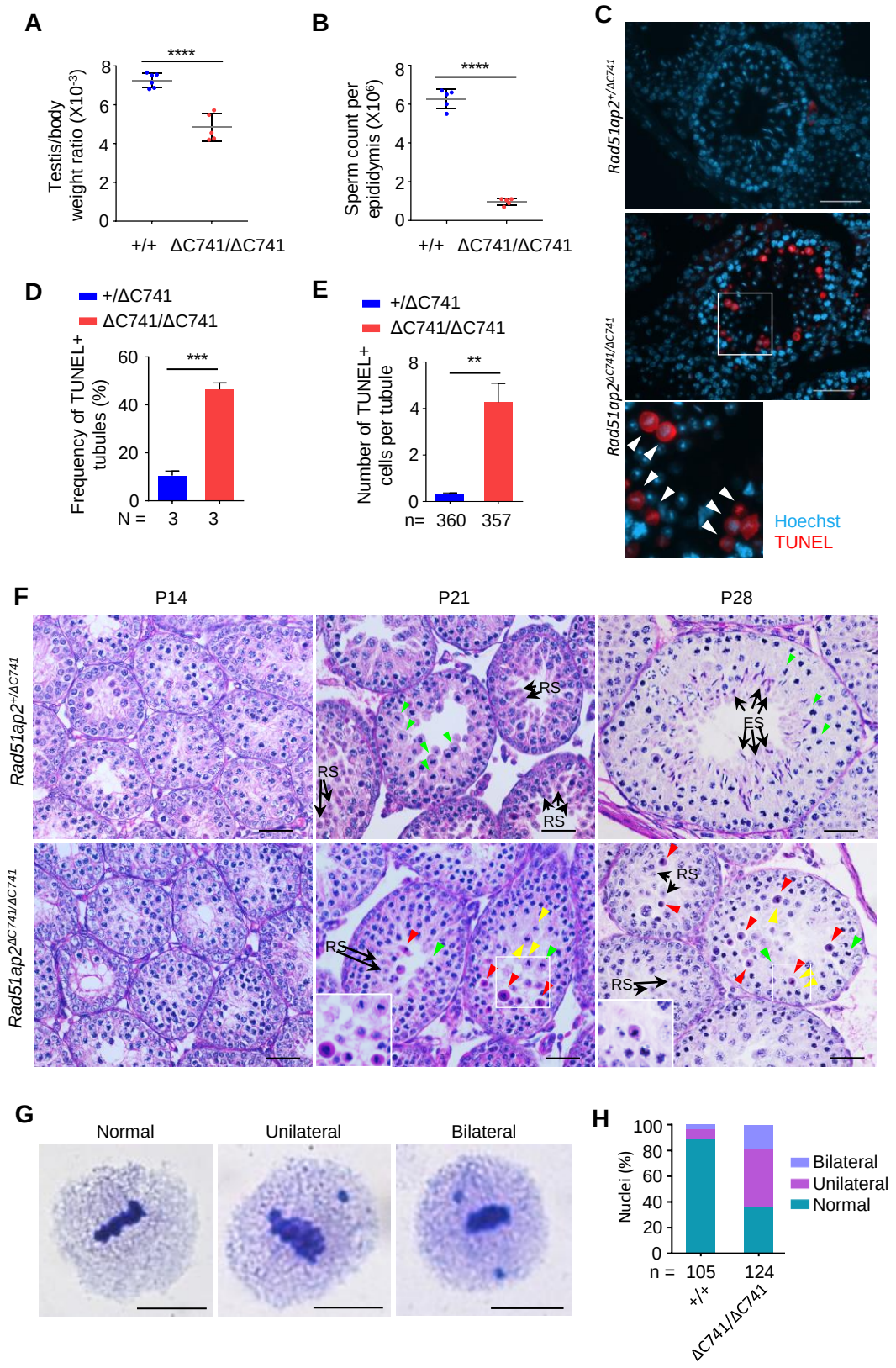

Fig. S4. Impaired spermatogenesis in *Rad51ap2* mutant mice. (**A-B**) Ratios of testis weight to body weight (**A**) and sperm count per epididymis (**B**) in 6-week-old WT and *Rad51ap2* mutant mice. Each dot represents the result from one mouse. ****P<0.0001; two-tailed Student's *t*-test. (**C**) Representative testicular sections stained for TUNEL (red). Hoechst 33342 (blue) labeled DNA. A magnified view of the box area is shown below. White arrowheads indicate apoptotic cells in metaphase. Scale bars, 50 μm. (**D**-**E**) Frequencies of TUNEL$^+$ tubules (**D**) and average numbers of TUNEL$^+$ cells per tubule (**E**). N, the number of mice scored. n, the number of tubules scored. **P<0.01, ***P<0.001; two-tailed Student's *t*-test. (**F**) PAS-stained testicular sections from control and *Rad51ap2* mutant mice at postnatal days (dpp) 14, 21 and 28. Green arrowheads indicate normal metaphase spermatocytes, red arrowheads indicate apoptotic meiotic metaphase I (MMI) spermatocytes, and yellow arrowheads indicate the unaligned chromosomes in MMI. Arrows indicate representative round spermatids (RS) or elongating/ed spermatids (ES). Scale bars, 50 μm. (**G**) Representative MMI spermatocytes with aligned or unaligned chromosomes. Scale bars, 50 μm. (**H**) Fractions of MMI spermatocytes with aligned chromosomes, unilateral or bilateral unaligned chromosomes in WT and *Rad51ap2*$^{\Delta C741/\Delta C741}$ mice. n, the number of cells scored.

Supplementary Figure 5

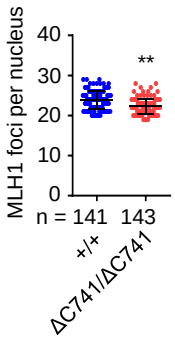

Fig. S5. Average numbers of MLH1 foci per nucleus. 141 WT spermatocytes and 143 mutant spermatocytes from three mice per genotype were scored. ***P*<0.01; two-tailed Student's *t*-test.

Supplementary Figure 6

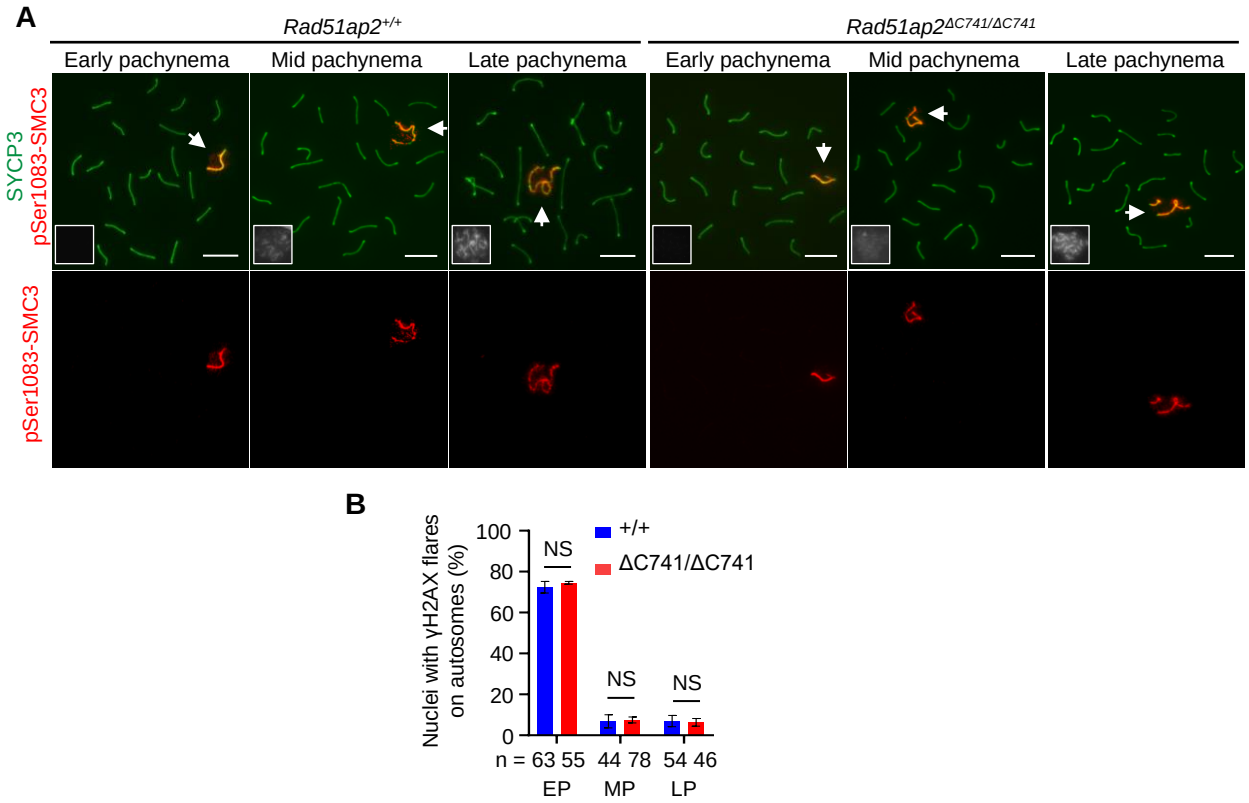

Fig. S6. No synapsis defects on autosomes were observed in *Rad51ap2* mutant spermatocytes. (**A**) Representative spread spermatocytes stained for SYCP3 (green), pSer1083-SMC3 (red, localizing on unsynapsed chromosomal regions but not with synapsed or desynapsed regions), and H1t (white). Arrows indicate the sex chromosomes. Miniaturized H1t staining (white) images are shown in the left-lower conner of the overlay images. Scale bars, 10 μm. (**B**) Percentages of spermatocytes with γH2AX flares on autosomes at indicated substages of pachytene as shown in (Fig. S7A). n shows the number of analyzed spermatocytes from two mice per genotype. NS, not significant (P>0.05); Two-way analysis of variance. EP, early pachynema. MP, mid pachynema. LP, late pachynema.

Supplementary Figure 7

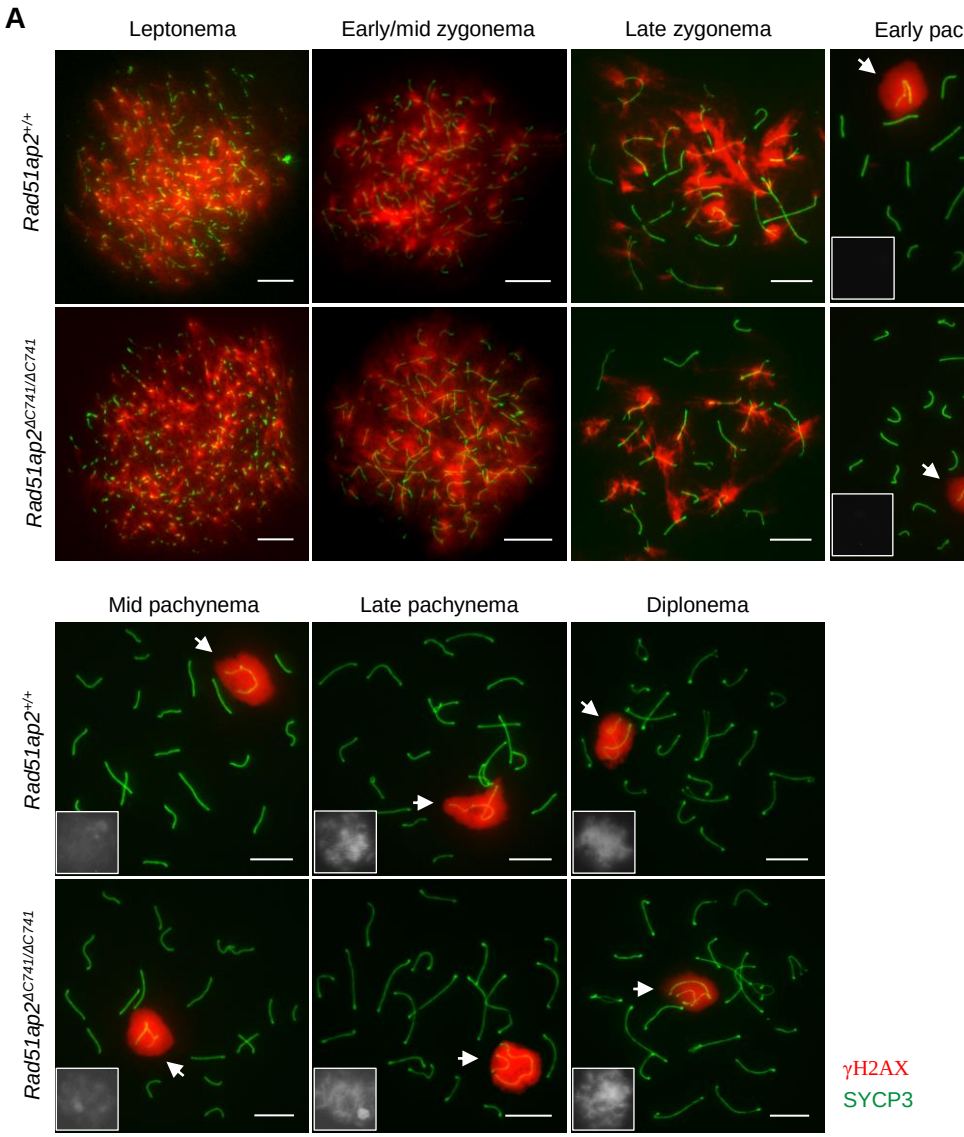

Fig. S7. Meiotic prophase progression analysis in *Rad51ap2* mutant male mice. (**A**) Representative spread spermatocytes from adult WT and *Rad51ap2* mutant mice stained for SYCP3 (green), γH2AX (red), and H1t (white). Miniaturized H1t staining images are shown in the left-lower corner of the overlay images of the pachytene and diplotene cells. Arrows indicate the sex chromosomes in pachytene and diplotene cells. Scale bars, 10 μm. (**B**) Frequencies of spermatocytes at successive stages of meiotic prophase I as shown in (**A**). n, the number of spermatocytes scored from at least two mice for each genotype. NS, not significant (P>0.05); Chi-square test.

Supplementary Figure 8

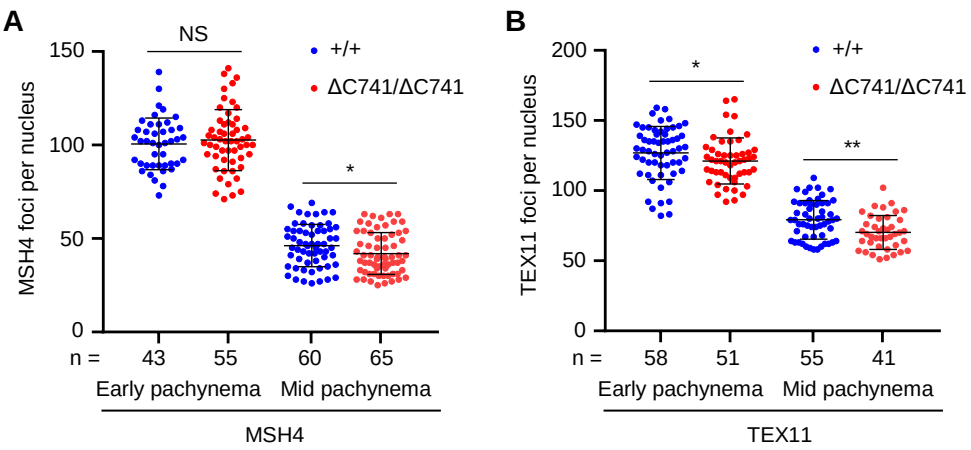

Fig. S8. Quantification of nucleus-wide MSH4 and TEX11 foci. The numbers of MSH4 and TEX11 foci per nucleus were counted in spread early and mid pachytene spermatocytes with XY touching. n, the number of spermatocytes scored from at least two mice per genotype. NS, not significant ($P>0.05$); *$P<0.05$; **$P<0.01$; Mann-Whitney U test.

Supplementary Figure 9

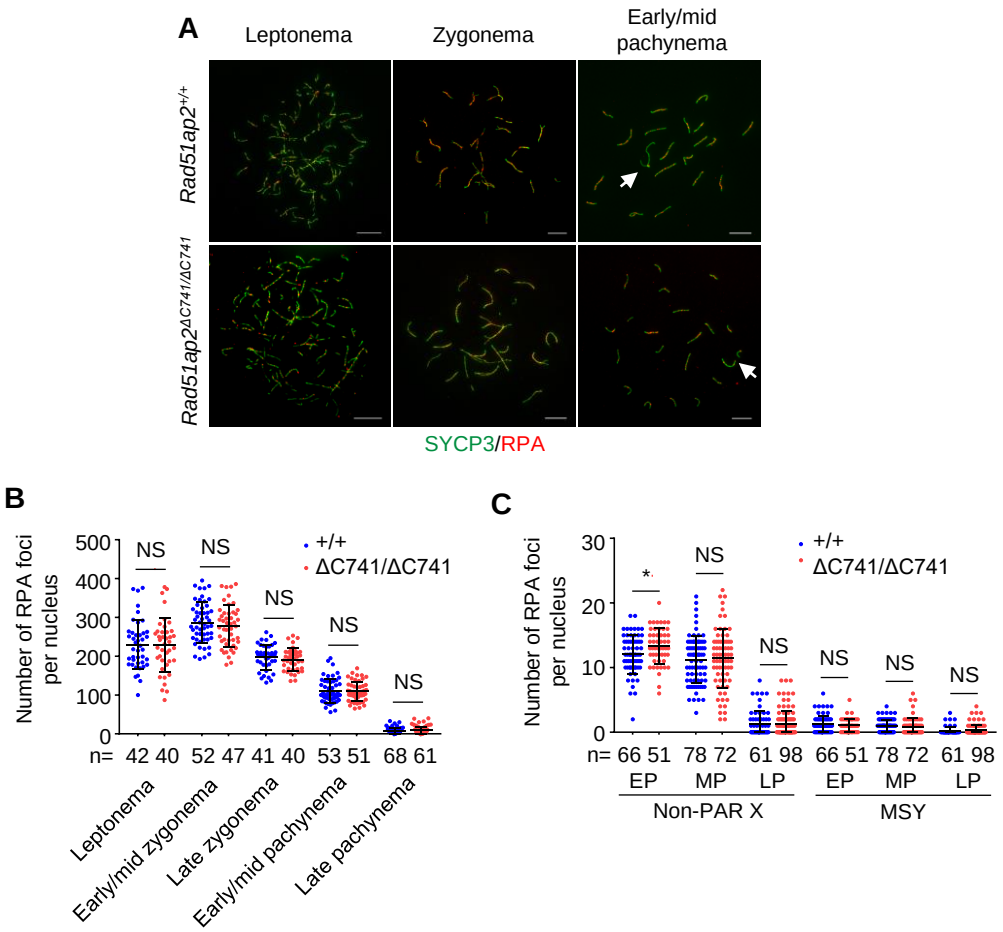

Fig. S9. Quantification of the dynamic changes of nucleus-wide RPA foci and RPA foci associated with non-PAR regions of the sex chromosomes. (**A**) Representative spread spermatocytes stained for SYCP3 (green) and RPA (red). Scale bars, 10 μm. (**B**) The numbers of RPA foci numbers in spread leptotene, early/mid zygotene, late zygotene, early/mid pachytene, and late pachytene spermatocytes from WT and *Rad51ap2* mutant mice. (**C**) The numbers of RPA foci on the chromosome axes along the X-specific region of X chromosome (termed as non-PAR X) and the male-specific region of Y chromosome (MSY) in pachytene spermatocytes. For (**B**) and (**C**), n, the number of spermatocytes scored from at least two mice per genotype. NS, not significant ($P>0.05$); *$P<0.05$; Mann-Whitney U test.

Supplementary Figure 10

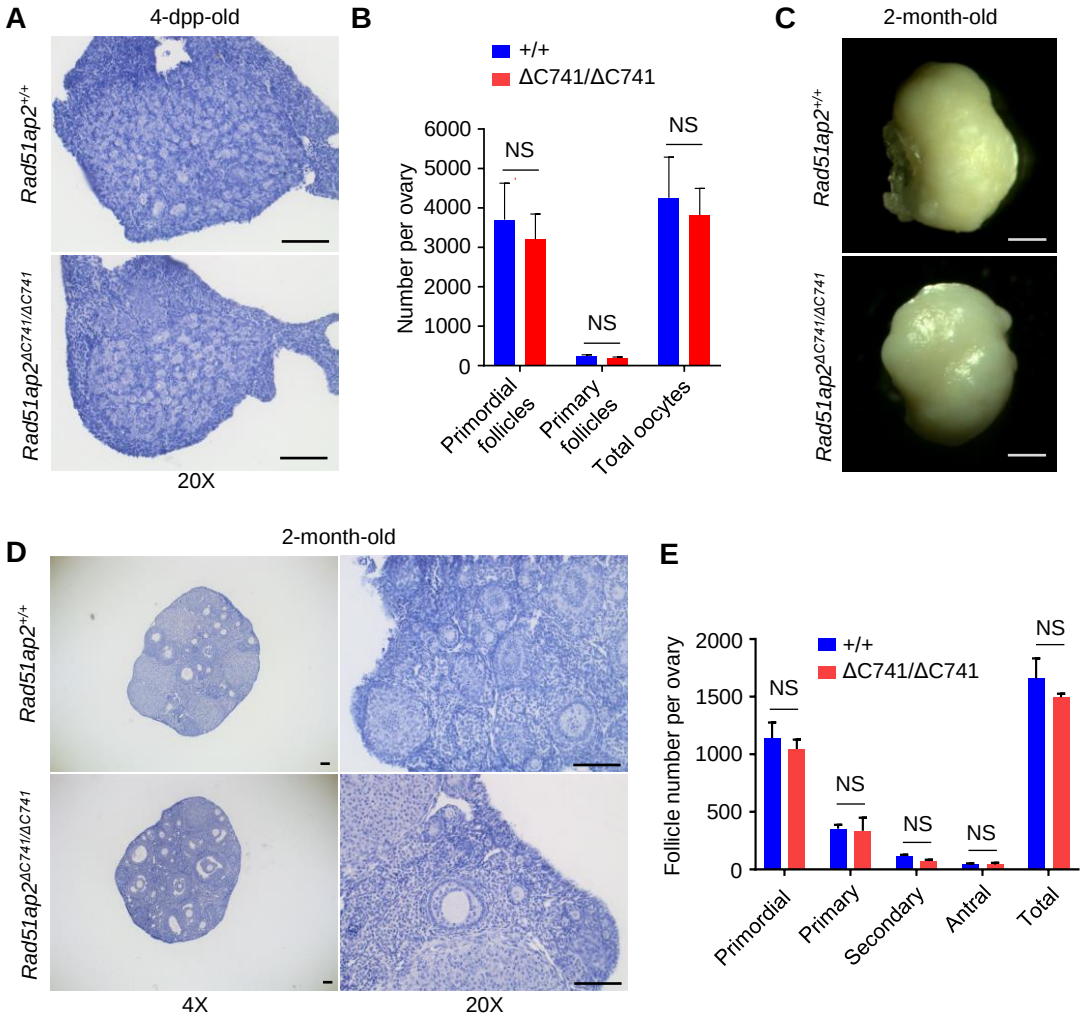

Fig. S10. Normal follicle development in the ovaries of *Rad51ap2* mutant mice. (**A,D**) Haemotoxylin staining results showing ovarian histology of 4-dpp-old (**A**) and 2-month-old (**D**) WT and *Rad51ap2* mutant mice. Scale bars, 100 μm. (**B,E**) Serial follicle counts and/or total oocyte counts in ovaries 4-dpp-old (**B**) and 2-month-old (**E**) WT and *Rad51ap2* mutant mice. Two ovaries from different females for each genotype at each indicated age were analyzed. NS, not significant; Two-way analysis of variance. Scale bars, 100 μm. (**C**) Morphologies of WT and *Rad51ap2* mutant ovaries at 2 months of age. Scale bars, 0.5 mm.

Supplementary Figure 11

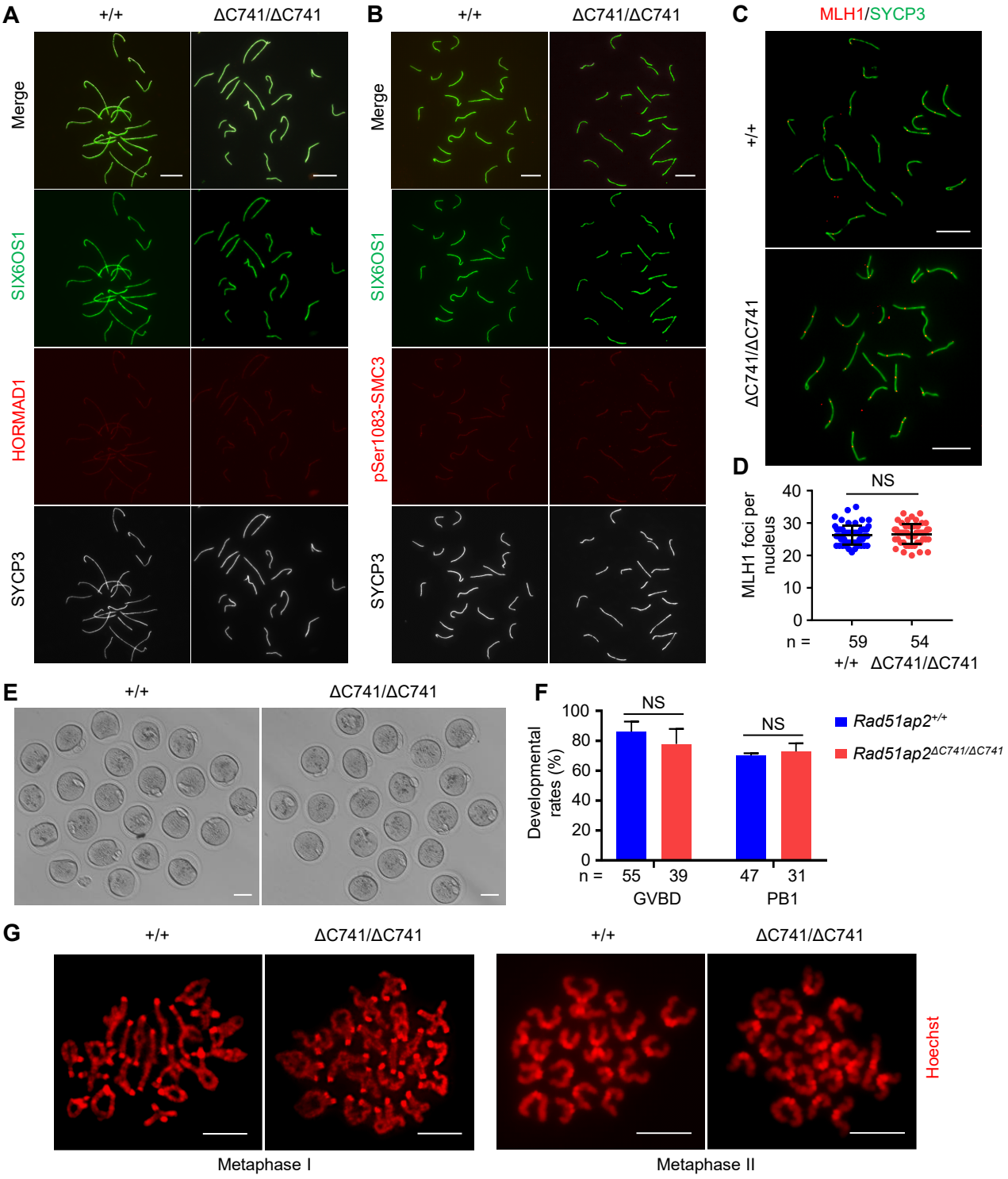

Fig. S11. No defects in synapsis, recombination, and meiotic maturation were observed in *Rad51ap2* mutant oocytes. (**A,B**) Representative spread oocytes from 17.5 days postcoitus (dpc) WT and *Rad51ap2* mutant fetal mice stained for SYCP3 (white) and SIX6OS1 (green), together with HORMAD1 (red, **A**) or pSer1083-SMC3 (red, **B**). Two mice were examined for each genotype. Scale bars, 10 μm. (**C**) Representative spread oocytes from 17.5 dpc WT and *Rad51ap2* mutant fetal mice stained for SYCP3 (green) and MLH1 (red). Scale bars, 10 μm. (**D**) Average MLH1 foci per nuclei. n, the number of oocytes scored from two mice per genotype. Student's *t*-test; NS, not significant. (**E**) Morphology of metaphase II oocytes under differential interference contrast microscopy after 16 hours of *in vitro* maturation culture. Fully grown germinal vesicle-stage oocytes were collected from permanent magnet synchronous generator-primed 3-week-old WT and *Rad51ap2*$^{\Delta C741/\Delta C741}$ mice and cultured *in vitro*. Scale bars, 50 μm. (**F**) The rates of germinal vesicle breakdown (GVBD) at 8 hours of culture and the rates of first polar body (PB1) extrusion at 16 hours of culture. n, the number of oocytes scored from three WT and two *Rad51ap2*$^{\Delta C741/\Delta C741}$ mice. NS, not significant; Two-way analysis of variance. (**G**) Representative images of chromosome spreads made from super-ovulated WT and mutant oocytes after *in vitro* maturation culture for 8 hours for metaphase I oocytes or 16 hours for metaphase II oocytes. DNA were labeled with Hoechst 33342 (red). All the WT (19 cells scored) and *Rad51ap2* mutant (10 cells scored) metaphase I oocytes examined had 20 bivalents, and all the WT (11 cells scored) and *Rad51ap2* mutant (7 cells scored) metaphase II oocytes examined had 20 chromosomes, each with two chromatids. Scale bars,10 μm.

Supplementary Figure 12

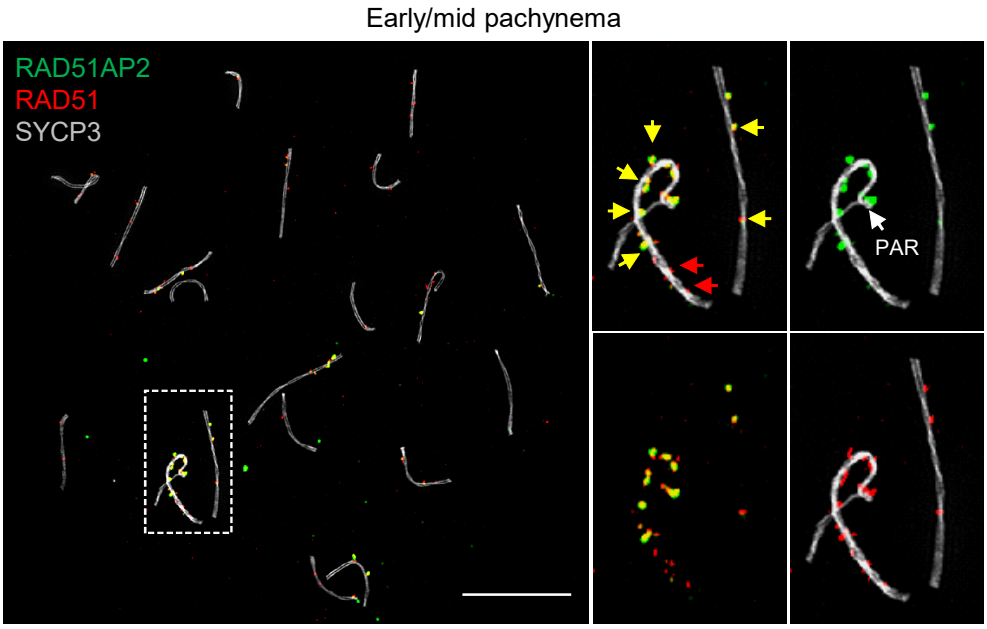

Fig. S12. Representative image showing co-localization of RAD51AP2 and RAD51 in early/mid pachynema. Representative images of WT early/mid pachytene spermatocyte nuclei stained for RAD51AP2 (green), RAD51 (red), and SYCP3 (gray) under structured illumination microscopy (SIM). Magnified views of the boxed areas are shown on the right. Yellow arrows indicate representative RAD51AP2 foci co-localizing with RAD51 and red arrows indicate representative RAD51 foci existing alone. The PAR is indicated by a white arrow. Scale bar, 10 μm.

Supplementary Figure 13

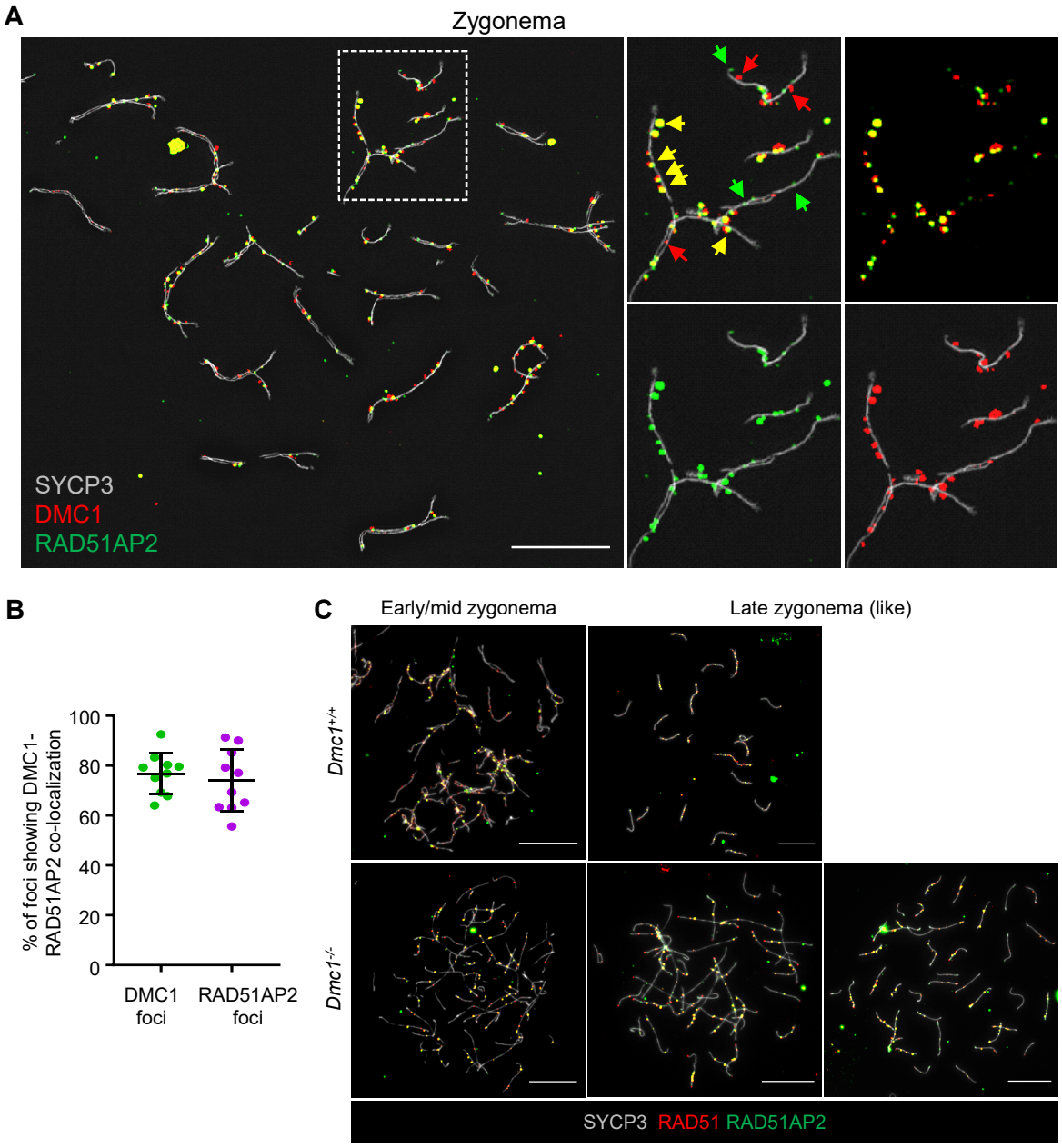

Fig. S13. **RAD51AP2 foci also co-localize with DMC1, but is independent of DMC1.** (**A**) Representative SIM images of WT spread spermatocytes stained for SYCP3 (gray), RAD51AP2 (green) and DMC1 (red) in late zygonema. Magnified views of the boxed areas are shown on the right. Yellow arrows indicate representative RAD51AP2 foci co-localizing with DMC1 (green and red signals overlap), red arrows indicate representative DMC1 foci existing alone, and green arrows indicate representative RAD51AP2 foci existing alone. (**B**) Ratios of DMC1-RAD51AP2 co-localizing foci to the DMC1 or RAD51AP2 total foci in zygotene spermatocytes under SIM. Foci from ten nuclei were quantified with each dot representing the ratio calculated from one nucleus. (**C**) Representative images of *Dmc1*$^{-/-}$ spermatocyte nuclei stained for RAD51AP2 (green), RAD51 (red), and SYCP3 (gray) under wide-field microscopy. Scale bas, 10 μm.

Supplementary Figure 14

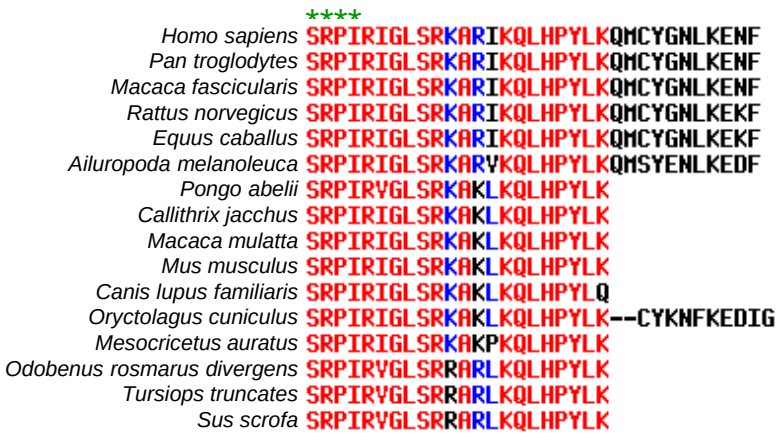

Fig. S14. Sequence alignment showing conservation of the RAD51AP2 C-terminus across different mammals. The alignment was performed using the online software MultAlin (http://multalin.toulouse.inra.fr/multalin/multalin.html). The SRPI residues are indicated by the asterisks.

Supplementary Figure 15

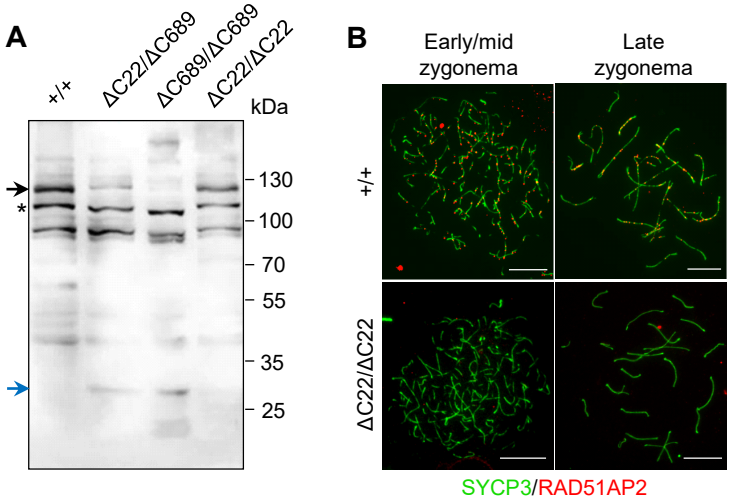

Fig. S15. The C-terminal 22 amino acids of mouse RAD51AP2 is required for its localization on chromosome axes. (**A**) Detection of RAD51AP2 proteins in testes from WT, *Rad51ap2*$^{\Delta C22/\Delta C689}$, *Rad51ap2*$^{\Delta C689/\Delta C689}$, and *Rad51ap2*$^{\Delta SRPI/\Delta SRPI}$ mice by Western blotting. Black arrow, the band corresponding to the WT RAD51AP2 proteins (predicted molecular weight, 112.2 kDa) or RAD51AP2 ΔC22 proteins (predicted molecular weight, 109.6 kDa). Blue arrow, the band corresponding to the RAD51AP2 ΔC689 proteins in the mutant mice. Asterisk, a non-specific band. (**B**) Representative spread spermatocytes stained for RAD51AP2 (red) and SYCP3 (green). Scale bars, 10 μm.

Supplementary Figure 16

A

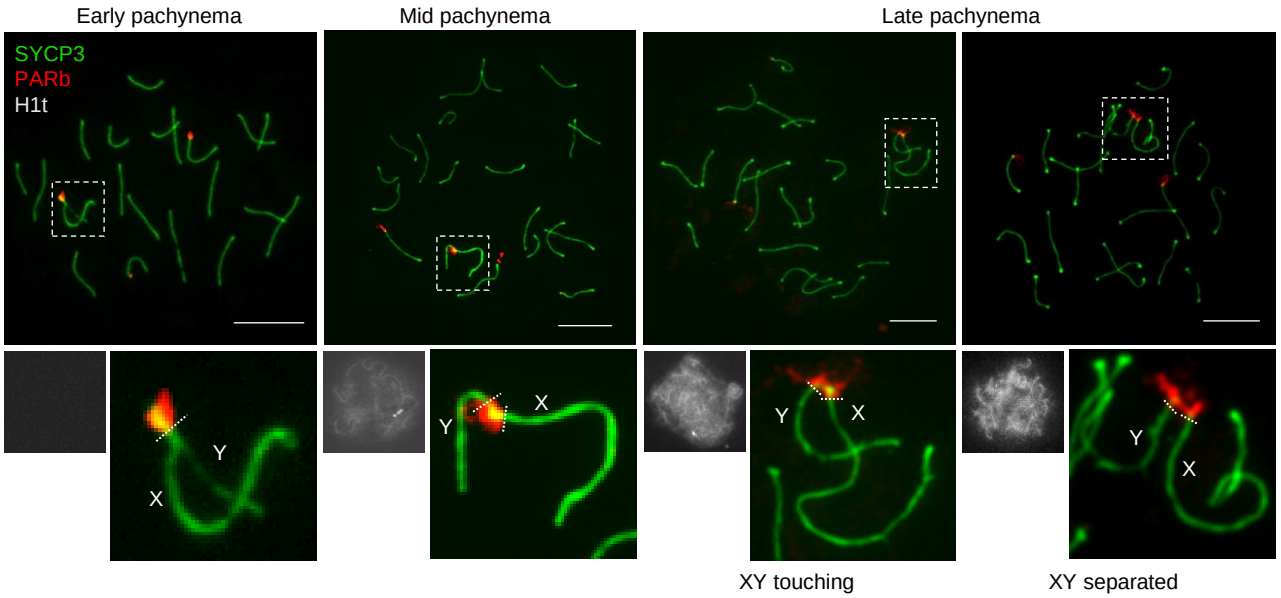

B

	X chromosome		Y chromosome	
Early pachynema	XY touching (n=24)	XY separated (n=12)	XY touching (n=24)	XY separated (n=12)
Total chr axis (μm, mean±SD)	10.32±1.45	10.43±1.81	4.41±1.15	4.34±1.40
PAR axis (μm, mean±SD)	0.59±0.20	0.44±0.12	0.70±0.22	0.62±0.14
Ratio of PAR axial length/ total chr axial length	0.057	0.042	0.160	0.142
Mid pachynema	XY touching (n=18)	XY separated (n=11)	XY touching (n=18)	XY separated (n=11)
Total chr axis (μm, mean±SD)	11.97±1.64	13.57±2.14	6.68±1.59	7.34±1.39
PAR axis (μm, mean±SD)	0.51±0.13	0.43±0.11	0.64±0.20	0.60±0.08
Ratio of PAR axial length/ total chr axial length	0.042	0.032	0.096	0.081
Late pachynema	XY touching (n=23)	XY separated (n=15)	XY touching (n=23)	XY separated (n=15)
Total chr axis (μm, mean±SD)	18.71±3.23	21.42±3.39	9.48±1.91	10.71±1.44
PAR axis (μm, mean±SD)	0.46±0.16	0.47±0.11	0.61±0.14	0.71±0.22
Ratio of PAR axial length/ total chr axial length	0.025	0.022	0.064	0.066

Fig. S16. Determination of the relative axial length of PARs in early, mid, and late pachynema. (**A**) Representative spread spermatocytes after staining with anti-SYCP3 antibodies (green) and PAR boundary FISH probes (PARb, red) which recognize PAR sequences that border the heterologous parts of X and Y chromosomes. Miniaturized H1t staining (white) image and magnified view of the sex chromosomes are shown below the overlay image. The axial length of PAR is measured from the axial tip to the PARb signals indicated by the dash line. Scale bars, 10 μm. (**B**) The ratios of the average PAR axial length to the average axial lengths of X and Y chromosomes in early, mid, and late pachynema. n, the number of nuclei scored.

Table S1. Clinical characteristics and biallelic *RAD51AP2* mutations identified by WES in patients.

	Reference values	**Case 241**		**Case 5809**	
Age (yr)[a]		26		34	
Height/weight (cm/kg) [a]		168/57		172/85	
Karyotype		46,XY		46,XY	
Right testis volume (ml) [b]	>12.5	10		12	
Left testis volume (ml) [b]	>12.5	10		12	
Semen analysis[b]					
Semen volume (ml)	>1.5	NA		6.87 ± 0.47	
Semen pH	>7.2	NA		7.23 ± 0.15	
Sperm count (10^6/ml)	>15	0		0	
Hormone analysis[c]					
Testosterone (ng/dl)	175-785	369.18		284.27	
Prolactin (ng/ml)	2.58-18.12	9.24		6.93	
Follicle-stimulating hormone (mIU/ml)	0.80-5.10	2.89		4.53	
Luteinizing hormone (mIU/ml)	1.24-8.62	8.42		3.00	
Oestradiol (pg/ml)	20-75	41.69		52.91	
RAD51AP2 mutations					
Mutation type		Compound heterozygous		Compound heterozygous	
Mutation at cDNA level		c.943_946del	c.3391insTTGGT	c.2191_2192del	c. 2484_2485del
Protein alteration		p.K315Lfs*2	p.R1131Lfs*19	p.V731Lfs*26	p.K828Nfs*4
Allele frequency in gnomAD		$4.07X10^{-6}$	0	0	$3.89X10^{-5}$
Allele frequency in ExAC		0	0	0	$5.10X10^{-5}$
Allele frequency in the 1000 Genomes		0	0	0	0
Allele frequency in ESP6500		0	0	0	0

[a] Age, height, and weight at sampling. [b] Reference values were published by WHO in 2010. [c] Reference values were suggested by clinical laboratory. NA, not available. Data are presented as mean ± SD for the semen analysis of case

5809. gnomAD, the Genome Aggregation Database. ExAC, the Exome Aggregation Consortium database. ESP6500, the exome sequencing project of > 6500 individuals by the National Heart, Lung and Blood Institute.

Table S2. Information of the primers.

Information	Name	Sequence
Primers for human gDNA amplification and Sanger sequencing	RAD51AP2 gDNA-Mut-1-F	AAAGAGGCATATGTTAGGGAT
	RAD51AP2 gDNA-Mut-1-R	GTGGTCAACAAAATACGTGC
	RAD51AP2 gDNA-Mut-2-F	GTCTAACGTTACAGTCCCAGT
	RAD51AP2 gDNA-Mut-2-R	CCTTGCTTTTCTTGACAAACC
	RAD51AP2 gDNA-Mut-3/4-F	AGTGCATGCTTTATTTGAAG
	RAD51AP2 gDNA-Mut-3/4-R	AGAAAACATGTCATCCATTG
Primers for TA-cloning of gDNA flanking the RAD51AP2-Mut-1 and Mut-2 in Case 241	Human gDNA amplification-F (F1 in Fig. S1a)	AAAGAGGCATATGTTAGGGAT
	Human gDNA amplification-R (R1 in Fig.S1a)	CCTTGCTTTTCTTGACAAACC
	Sanger sequencing (F2 in Fig.S1a)	AAGTGCCACCTGACGTCTAA
	Sanger sequencing (R2 in Fig.S1a)	GAAGAGCGCCCAATACGCAA
Primers for genotyping of the *Rad51ap2* mutant mice	ΔC689/ΔC689-F	AGCAGAAGTGAGTCATGCTC
	ΔC689/ΔC689-R	TAGATCTGTCACAGTCCAAG
	ΔC741/ΔC741-F	AGCAGAAGTGAGTCATGCTC
	ΔC741/ΔC741-R	TAGATCTGTCACAGTCCAAG
	ΔSRPI/ΔSRPI-F	TTGTCCTCTTTGCAGGCAGT
	ΔSRPI/ΔSRPI-R	TGAAGCTGTTTCAGCCTAGC
	ΔC22/ΔC22-F	ATGGCAGAGTTGCTTCCCTT
	ΔC22/ΔC22-R	ACAAAATCTGCAGCTGGAGG
Primers for constructing plasmids for Co-IP	Flag-RAD51-F	GATTACAAAGACGATGACGATAAAAT GGCAATGCAGATGCAGC
	Flag-RAD51-R	GATTACAAAGACGATGACGATAAATC AGTCTTTGGCATCTCCCACTCC
	GFP-RAD51AP2-WT-F	TCGAGCTCAAGCTTCGAATTCATGTCT CTCCCTCAGCCCAC
	GFP-RAD51AP2-WT-R	ATGGTGGCGACCGGTGGATCCCGAAA ATTTTCTTTTAAGTTTCCGTAACAC
	GFP- RAD51AP2-Mut-2-F	GCATGGACGAGCTGTACAAGATGTCT CTCCCTCAGCCCAC
	GFP- RAD51AP2-Mut-2-R	GATCTAGAGTCGCGGCCGCTTCAAAA ATTTTCTTTTAAGT

Table S3. Information of the antibodies.

Name of antibodies	Host	Company	Catalog number or antigens[a]	Dilution
SYCP3	Mouse	Abcam	ab97672	IF: 1:200
	Rabbit	Novus Biologicals	NB300-231	IF: 1:500
MLH1	Mouse	BD Pharmingen	551092	IF: 1:50
γH2AX	Rabbit	Novus Biologicals	NB100-384	IF: 1:5000
	Mouse	Millipore	05636	IF: 1:250
RAD51AP2	Rabbit	Customizedly produced by ABclonal	87-326 aa and 131-320 aa, respectively	IF: 1:800 WB: 1:4000
	Rat	Customizedly produced by ABclonal		IF: 1:500 WB: 1:3000 IP: 1:500
RAD51	Rabbit	Customizedly produced by ABclonal	1-92 aa	WB: 1:2000
	Guinea pig	Customizedly produced by ABclonal	1-92 aa	IF: 1:100 IP: 1:500
	Rabbit	Santa Cruz	sc-8349	IF: 1:200
DMC1	Guinea pig	Customizedly produced by ABclonal	1-100 aa	IF: 1:100
RPA1	Rabbit	Gift from Prof. P. Jeremy Wang	-	IF: 1:100
H1t	Guinea pig	Customizedly produced by Dia-An Biotech	113-209 aa	IF: 1:800
SIX6OS1	Rabbit	Customizedly produced by Youke	5-268 aa	IF: 1:800
pSer1083-SMC3	Rabbit	Bethyl	A304-637A	IF: 1:200
HORMAD1	Rabbit	Proteintech	13917-I-AP	IF: 1:500
MSH4	Rabbit	Abcam	ab58666	IF: 1:100
TEX11	Rabbit	Gift from Prof. P. Jeremy Wang	-	IF: 1:100
CREST	Human	Immunovision	HCT-0100	IF: 1:500
β-Actin	Rabbit	Abcam	ab8227	WB: 1:3000
GFP	Mouse	Abmart	M20004	WB: 1:3000 IP: 1:500
Monoclonal anti-Flag	Mouse	Sigma	F1804	WB: 1:2000 IP: 1:1000
Normal Rabbit IgG	Rabbit	Cell Signaling Technology	#2729	IP: 1:500
Alexa Fluor® 555 Donkey anti-Rabbit IgG (H+L)	Donkey	Molecular Probes	A-31572	IF: 1:200
Alexa Fluor® 488 Goat anti-Mouse IgG1	Goat	Molecular Probes	A-21121	IF: 1:100
Alexa Fluor® 488 Goat anti-Rat IgG (H+L)	Goat	Molecular Probes	A-11006	IF: 1:100

Alexa Fluor® 647 Goat anti-Mouse IgG (H+L)	Goat	Molecular Probes	A-21235	IF: 1:200
Alexa Fluor® 647 Goat anti-Rabbit IgG (H+L)	Goat	Molecular Probes	A-21244	IF: 1:200
Alexa Fluor® 647 Goat anti-Guinea Pig IgG (H+L)	Goat	Molecular Probes	A-21450	IF: 1:200
Fluorescein (FITC)-conjugated Affinipure Donkey	-	Jackson ImmunoResearch Inc.	706-095-148	IF: 1:100
HRP Donkey anti-rabbit IgG	Donkey	BioLegend, Inc	406401	WB: 1:10000
HRP Goat anti-rat IgG	Goat	BioLegend, Inc	405405	WB: 1:10000
HRP Goat anti-mouse IgG	Goat	BioLegend, Inc	405306	WB: 1:10000

[a]antigen information was shown for customizedly produced antibodies, rather than catalog number. IP, immunoprecipitation. WB, Western blotting. IF, immunofluorescence staining.